is predicted by McConnell for the addition of a single carbon–carbon σ-bond between two paramagnetic centers,[42] which was experimentally verified for some diradicals.[37c,43] But the J value for **5** still complies with the condition of $|J| \gg |a_{iso}(^{51}V)|$, required for equal coupling of the two unpaired electrons with both V centers.[43]

The relatively large exchange integral in **2** compared with exchange interactions in fulvalene[44] and biphenyl-bridged dinuclear complexes, wherein the metal centers possess less than 18 ve,[25b,38,45] causes the assumption that generally stronger exchange interactions occur in complexes containing ligand systems which can be formally described as one polyene ligand linking two metal centers (structure II).

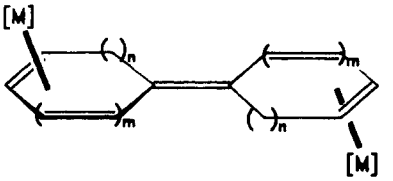

n = 0, 1...
m = 0, 1, 2...

II

Acknowledgment. We are greatly indebted to BASF for a donation of Cot and to the Fonds der Chemischen Industrie, Germany, for financial support.

Supplementary Material Available: A figure showing solid-solution X-band ESR spectra of **4** and **5** as well as a solid-solution Q-band spectrum of **5** (Figure 3D–F) and tables giving V–C and C–C bond lengths and angles of the CpV fragments and C–H bond lengths of **2** and **5** (Table 6), final fractional atomic coordinates and coefficients of isotropic thermal displacement factors of the hydrogen atoms (Table 7), anisotropic thermal displacement factors (Tables 8 and 9), and weighted least-squares planes through the cyclooctatrienyl ligands and equations of the planes (7 pages); tables of observed and calculated structure factors (27 pages). Ordering information is given on any current masthead page.

(42) McConnell, H. M. *J. Chem. Phys.* **1960**, *33*, 115.
(43) Briere, R.; Dupeyre, M. R.; Lemaire, H.; Morat, C.; Rassat, A.; Rey, P. *Bull. Soc. Chim. Fr.* **1965**, 3290. Dupeyre, M. R.; Lemaire, H.; Rassat, A. *J. Am. Chem. Soc.* **1965**, *87*, 3771. Glarum, S. H.; Marshall, J. H. *J. Chem. Phys.* **1967**, *47*, 1374.
(44) Schwarzhans, K. E.; Schottenberger, H. *Z. Naturforsch., B* **1983**, *38*, 1493 and literature cited therein. Sharp, P. R.; Raymond, K. N.; Smart, J. C.; McKinney, R. J. *J. Am. Chem. Soc.* **1981**, *103*, 753 and literature cited therein.
(45) For biphenyl-bridged dinuclear η^6-arene complexes consisting of 17 valence electrons on each metal center (see refs 25b, 38) the exchange parameter J is estimated from the temperature-dependent intensity of the half-field signal $\Delta m_s = 2$: $0 > J > -10$ cm^{-1} (Elschenbroich, Ch.; Heck, J. Unpublished results). For **2** a corresponding estimation of J leads to $J = -80 \pm 5$ cm^{-1}, which is in good agreement with the J value obtained from the susceptibility measurements.

Contribution from the Department of Chemistry,
Iowa State University, Ames, Iowa 50011

Two Novel Phases Containing Centered, Isolated Zirconium Clusters, $Rb_4Zr_6Cl_{18}C$ and $Li_6Zr_6Cl_{18}H$

Jie Zhang, Robin P. Ziebarth, and John D. Corbett*

Received August 6, 1991

The title compounds are synthesized by reaction of Zr, $ZrCl_4$ with RbCl plus graphite, or LiCl plus $ZrH_{1.7}$ at ~850 or 700 °C, respectively. Stability of the rubidium phase is marginal, and the synthesis requires excess zirconium. The structures of the two have been established by single-crystal X-ray diffraction: $Rb_4Zr_6Cl_{18}C$, $K_4Nb_6Cl_{18}$ type, $C2/m$, $Z = 2$, $a = 10.460$ (4) Å, $b = 17.239$ (4) Å, $c = 9.721$ (4) Å, $\beta = 115.05$ (3)°, $R(F)/R_w = 2.4/3.3\%$; $Li_6Zr_6Cl_{18}H$, $R\bar{3}$, $Z = 3$, $a = 15.969$ (1) Å, $c = 8.883$ (1) Å, $R(F)/R_w = 2.2, 2.5\%$. Individual close-packed layers of isolated $\{Zr_6(C)Cl^i_{12}Cl^a_6\}^{4-}$ clusters are present in the rubidium salt. However, the requirement of four cation sites results in offset, not close, packing of the layers, and the cations between these are bound more tightly to one layer than the other. The exo Zr–Cl^a bonds (2.59 Å) are the shortest known because of weaker Cl^a···Rb interactions. The rhombohedral $Li_6Zr_6Cl_{18}H$ contains cubic-close-packed $\{[Zr_6(H)Cl^i_{12}]Cl^a_6\}^{6-}$ clusters with lithium in pseudooctahedral cavities between and within the layers. The Zr–cluster center distance, 2.257 Å, is at least 0.16 Å too large for good bonding of the hydride, and the solid-state ^{1}H NMR shift (~400 ppm vs Fe^{3+}(aq) at room temperature) is similar to that in $Zr_6Cl_{12}H$ where a high hydrogen mobility is present. The sharp 11.8 ppm absorption in the ^{7}Li NMR spectrum (relative to LiCl) is consistent with the site symmetry deduced by X-ray diffraction and the nature of the nearest-neighbor chlorine atoms.

Introduction

The large collection of centered zirconium chloride cluster compounds $A_xZr_6(Z)Cl_{12}Cl_n$ owe their diversity to several factors. A considerable electronic variability is allowed by choices of both the number of valence electrons on the centering interstitial Z and the number (and charge) of the countercations within the cluster structure. A third variable provides the great structural variety exhibited by these compounds (as well as an electronic parameter), namely, the $0 \le n \le 6$ additional chlorine atoms that may be utilized in the essential Zr–Cl^a bonding exo to all six metal vertices of each $Zr_6(Z)Cl^i_{12}$ cluster unit. The sharing of chlorine atoms in this role between clusters necessarily joins these into network structures for all but for the limiting $n = 6$, where discrete $Zr_6(Z)Cl^i_{12}Cl^a_6$ (=$Zr_6Cl_{18}Z$) units pertain (i = inner, edge bridging; a = exo, terminal chlorine). The variables x, Z, and n thus afford numerous ways in which one can achieve, or come close to, the most favorable counts of cluster-based electrons, 14 with main-group (s, p) and 18 with transition-metal (d) interstitials in zirconium chloride clusters.[1-4]

The present article describes two of a small number of $A_xZr_6Cl_{18}Z$ phases known. Previous examples have been only $Rb_5Zr_6Cl_{18}B$[2] and an uncommon alkaline-earth-metal member, $Ba_3Zr_6Cl_{18}Be$,[5] although the $Zr_6Cl_{18}Z$ units in the latter are not quite as independent because of the higher charged cations. In fact, the latter compound is a proper member of a series $M_2M'Cl_6{\cdot}Zr_6Cl_{12}Z$[6] (=$M_2M'Zr_6Cl_{18}Z$) in which each $Zr_6Cl_{12}Z$ cluster is bridged to others via six $M'Cl_6$ octahedra bonded at the exo positions. The original examples $M_2ZrCl_6{\cdot}Zr_6Cl_{12}H$ with M = Na–Cs[7] thus contain $Zr_6Cl_{12}H$ clusters interconnected by

(1) Ziebarth, R. P.; Corbett, J. D. *Acc. Chem. Res.* **1989**, *22*, 256.
(2) Ziebarth, R. P.; Corbett, J. D. *J. Am. Chem. Soc.* **1989**, *111*, 3272.
(3) Rogel, F.; Zhang, J.; Payne, M. W.; Corbett, J. D. *Adv. Chem. Ser.* **1990**, *No. 226*, 369.
(4) Zhang, J.; Corbett, J. D. *Inorg. Chem.* **1991**, *30*, 437.
(5) Zhang, J.; Corbett, J. D. *Z. Anorg. Allg. Chem.* **1991**, *599/600*, 381.
(6) Zhang, J.; Corbett, J. D. To be submitted for publication.

0020-1669/92/1331-0614$03.00/0

$ZrCl_6^{2-}$ units, the tight bonding of the latter making the categorization of $Zr_6Cl_{18}H$ units therein quite ambiguous. In contrast, $Rb_4Zr_6Cl_{18}C$ reported here occurs in a unique structure type defined by the first M_6X_{18} cluster example reported, $K_4Nb_6Cl_{18}$,[8] although the new analogue also exhibits some uncommon stability problems.

The new $Li_6Zr_6Cl_{18}H$ is also a member of a small family of hydrogen-centered clusters. All others were originally obtained through the unanticipated intervention of hydrogen as the necessary cluster-stabilizing interstitial and were later established as hydrides by their direct, high-yield syntheses.[9] Two of these, $Zr_6X_{12}H$ with X = Cl or Br, have been characterized as $Zr_6I_{12}C$ type[10] only by X-ray powder diffraction, while just the foregoing $K_2ZrCl_6 \cdot Zr_6Cl_{12}H$ (=$K_2Zr_7Cl_{18}(H)$) has been characterized by single-crystal X-ray diffraction.[7] A particularly interesting feature of both of these hydride structure types is that the cavity size is evidently determined largely by Zr–Zr interactions and as such is oversized for hydrogen,[11] by about 0.17 Å in d(Zr–H) in the last phase. The "rattling" of hydrogen in $Zr_6Cl_{12}H$ and the paramagnetic nature of the cluster have been demonstrated by solid-state NMR measurements.[12] Difficulties in securing any of the foregoing cluster hydrides in greater than 80–90% purity and a desire to examine further the novel nature of the loosely bound hydrogen in such has led us to explore other systems. In the new $Li_6Zr_6Cl_{18}H$, the packing of clusters without direct interconnections is dominant in determining the three-dimensional structure, and high lithium content also makes it an ideal compound for ^7Li solid-state NMR studies. The acidity of these cations is probably a major factor in making the compound a good reagent for nonaqueous solution reactions as well.[13]

Experimental Section

The preparation of powdered Zr and $ZrCl_4$ from crystal bar material, the reaction techniques utilizing welded Ta containers, and the Guinier powder diffraction procedures were as previously described.[2,4,9] All materials were handled only in a glovebox containing <1 ppm H_2O by volume.

Syntheses. $Rb_4Zr_6Cl_{18}C$ was first produced as well-crystallized ruby-colored hexagonal prisms via a reaction of a mixture of Zr powder, $ZrCl_4$, RbCl, and graphite with the stoichiometry of the hypothetical $Rb_3Zr_6Cl_{15}C$ (850 °C, 14 days). But the quantitative synthesis of this compound turned out to be nontrivial even though a structure determination with these crystals succeeded without any difficulties. Products of reactions loaded to reproduce the $Rb_4Zr_6Cl_{18}C$ stoichiometry and run under conventional conditions (800–850 °C, 14–20 days) were a uniform black color and appeared to be crystalline under an optical microscope. However, they were, surprisingly, largely amorphous, most of the X-ray powder patterns showing only broad lines of Rb_2ZrCl_6 (K_2PtCl_6 type) plus fewer than 10 weak reflections for $RbZr_6Cl_{15}C$[14] (estimated yield <10%). Non-water-based mounting tape did not provide better patterns, implying that the problem existed prior to the X-ray sample mounting. Slow cooling, annealing, or changing the reaction stoichiometry back to that for $Rb_3Zr_6Cl_{15}C$ failed to alter the results. On the basis of experience, it is believed that the desired product $Rb_4Zr_6Cl_{18}C$ does form during the reaction, since a failed reaction usually affords a well-crystallized sample of an alternate cluster phase (e.g. $RbZr_6Cl_{15}C$) in reasonable yield (>70%). The problem is not understood, but $Rb_4Zr_6Cl_{18}C$ appears to decompose at a relatively low temperature into crystalline and other unidentified phases that give only broad lines at low values of θ. Present observations suggest that the problem originates not with the stability of the $Zr_6Cl_{12}C^{2+}$ cluster, which has the normal 14-electron count, but with the lattice (below).

A surprising success was the good diffraction pattern as well as nicely formed crystals of $Rb_4Zr_6Cl_{18}C$ encountered after a typical product (which had been annealed at lower temperatures) was reacted with ample excess Zr powder ($Rb_4Zr_6Cl_{18}C$:Zr = 1:2) at 850 °C for 20 days. The yield was 80–90%, with ZrCl as the only other halide. Other examples where excess metal is necessary for stability have been noted before, including for $Rb_5Zr_6Cl_{18}B$.[2] There appear to be related potassium and sodium analogues of the rubidium phase with similar stability problems. Efforts to replace the interstitial carbon by the "isoelectronic" iron yielded mainly $MZr_6Cl_{15}Fe$ (M = Rb, Cs; $CsNb_6Cl_{15}$ type[6]) and M_2ZrCl_6.

Table I. Selected Crystal and Refinement Information

compd	$Rb_4Zr_6Cl_{18}C$	$Li_6Zr_6Cl_{18}H$
space group, Z	$C2/m$ (No. 12), 2	$R\bar{3}$ (No. 148), 3
a,[a] Å	10.460 (4)	15.969 (1)
b, Å	17.239 (4)	15.969 (1)
c, Å	9.721 (4)	8.883 (1)
β, deg	115.05 (3)	(90)
V, Å^3	1588.0 (9)	1961.7 (4)
abs coeff μ, cm^{-1} (Mo Kα)	93.5	41.3
range of transm coeff	0.68–1.00	0.93–1.00
R,[b] %	2.4	2.2
R_w,[c] %	3.3	2.5

[a] From Guinier powder diffraction with Si as an internal standard and 42 and 38 data, respectively; λ = 1.540 562 Å. [b] $R = \sum||F_o| - |F_c||/\sum|F_o|$. [c] $R_w = [\sum w(|F_o| - |F_c|)^2/\sum w(F_o)^2]^{1/2}$; $w = [\sigma(F)]^{-2}$.

$Li_6Zr_6Cl_{18}H$ was first discovered following a reaction of Zr, $ZrCl_4$, LiCl, and $ZrH_{1.7}$ that was targeted at $Li_2Zr_6Cl_{12}H$, a phase which would contain a 14-electron cluster. A black powder and several dark red crystals were obtained after 2 weeks at 700 °C, and the powder pattern showed approximately equal amounts of $Zr_6Cl_{12}H$, the new cluster hydride, ZrO_xH_yCl,[15] and at least one other phase that remains unidentified. Following the structural characterization of one of the single crystals noted above, $Li_6Zr_6Cl_{18}H$ was obtained in high yield (>90% plus small amounts of ZrCl and $ZrCl_4$) from reactions with the correct stoichiometry. No significant changes in the cell parameters were observed when the starting Li and H proportions were varied, indicating that $Li_6Zr_6Cl_{18}H$ is a line compound. It should be emphasized that omission of just the hydrogen component eliminates all reduced cluster products, giving only $ZrCl_n$, LiCl, etc. instead. A specific test of the lithium content with a reaction run with only 80% of the theoretical amount of that element produced a lower yield of the same phase with essentially the same lattice constants plus ZrCl and $ZrCl_4$. An attempt to increase the Li:Zr ratio to 7:6 and to synthesize a 14-electron cluster in $Li_7Zr_6Cl_{18}H$ was unsuccessful. Moreover, attempts at partial or complete substitution of Li with Na or replacement of H with Be also failed, these producing 50% of an unknown phase in the former and $LiZr_6Cl_{14}Be$[9] in the latter.

Larger quantities of $Li_6Zr_6Cl_{18}H$ and $Li_6Zr_6Cl_{18}D$ were prepared for vibration spectral studies by inelastic neutron scattering.[16] Duplicate reactions were loaded in welded Ta tubes of 1.5 × 8 cm size, each containing up to 1.8 g of the starting materials. The reactions were slowly heated to 700 °C in 1 week and maintained at this temperature for over 4 weeks. The ends of the Ta containers were usually slightly bulged after the reaction, indicating a significant pressure had developed in the course of the reaction. The estimated yields were at least 95%, and the only detectable impurity was ZrO_xH_yCl, similar to what has been observed in the $Zr_6Cl_{12}H$ system.[9,12]

Structure Determinations. $Rb_4Zr_6Cl_{18}C$. Diffraction data were collected at room temperature with the aid of an Enraf-Nonius CAD 4 diffractometer. The primitive triclinic cell obtained through indexing of 25 reflections transformed to a standard C-centered monoclinic cell. A mirror plane perpendicular to the b direction was indicated by axial photographs, and an additional picture taken along the [110] direction confirmed the Laue symmetry. One hemisphere of data was collected with the C-centering condition. The data preparation included a nonlinear decay correction for an unusual 9% intensity loss during the 53-h X-ray exposure and an empirical absorption correction with the aid of the average of seven ψ-scans. Other information on data collection and refinement is summarized in Table I.

The initial model provided by SHELXS-86[17] refined well by standard least-squares methods, ultimately anisotropically. At this stage the interstitial carbon was located on a difference Fourier map. The occupancies of C and Rb were also refined but thereafter held at unity since they did not significantly differ therefrom (C, 98 (2)%; Rb, 100.1 (1)%). The final difference Fourier map contained no positive or negative peaks

(7) Imoto, H.; Corbett, J. D.; Cisar, A. *Inorg. Chem.* **1981**, *20*, 145.
(8) Simon, A.; von Schnering, H.-G.; Schäfer, H. *Z. Anorg. Allg. Chem.* **1968**, *361*, 235.
(9) Ziebarth, R. P.; Corbett, J. D. *J. Solid State Chem.* **1989**, *80*, 56.
(10) Smith, J. D.; Corbett, J. D. *J. Am. Chem. Soc.* **1985**, *107*, 5704.
(11) Wijeyesekera, S. D.; Corbett, J. D.; *Inorg. Chem.* **1986**, *25*, 4709.
(12) Chu, P. J.; Ziebarth, R. P.; Corbett, J. D.; Gerstein, B. C. *J. Am. Chem. Soc.* **1988**, *110*, 5324.
(13) Rogel, F.; Corbett, J. D. *J. Am. Chem. Soc.* **1990**, *112*, 8198.
(14) Ziebarth, R. P.; Corbett, J. D. *J. Am. Chem. Soc.* **1987**, *109*, 4844.
(15) Seaverson, L. M.; Corbett, J. D. *Inorg. Chem.* **1983**, *22*, 3203.
(16) White, R. P.; Kearley, G. K.; Eckert, J. Private communications.
(17) Sheldrick, G. M. SHELXS-86, *Programs for Structure Determination*, Universität Göttingen, Germany, 1986.

Table II. Positional and Isotropic Thermal Parameters for $Rb_4Zr_6Cl_{18}C$ and $Li_6Zr_6Cl_{18}H$

	x	y	z	B_{eq},[a] Å^2
		$Rb_4Zr_6Cl_{18}C$		
Zr1	0.12273 (5)	0	0.85252 (5)	2.10 (1)
Zr2	0.14648 (4)	0.09366 (3)	0.15148 (4)	2.102 (7)
Cl1	0.3265 (2)	0	0.3325 (2)	2.84 (3)
Cl2	0	0.2078 (1)	0	3.05 (3)
Cl3	0.2981 (1)	0.10448 (7)	0.0053 (1)	3.11 (2)
Cl4	0.0256 (1)	0.10443 (7)	0.3266 (1)	2.86 (2)
Cl5	0.2625 (2)	0	0.6903 (2)	3.62 (4)
Cl6	0.3134 (1)	0.20005 (8)	0.3266 (1)	3.37 (2)
Rb	0.39310 (5)	0.16175 (4)	0.68488 (6)	4.26 (1)
C	0	0	0	2.1 (2)
		$Li_6Zr_6Cl_{18}H$		
Zr	0.10662 (2)	0.12293 (2)	0.14606 (3)	0.89 (1)
Cl1	0.52716 (6)	0.31435 (6)	0.00273 (9)	1.33 (4)
Cl2	0.10153 (6)	0.25834 (6)	0.00089 (9)	1.34 (3)
Cl3	0.43807 (6)	0.06773 (6)	0.00322 (9)	1.41 (4)
Li	0.0586 (6)	0.4932 (6)	0.160 (1)	3.7 (3)
H[b]	0	0	0	

[a] $B_{eq} = ((8\pi^2)/3)\sum_i\sum_j U_{ij}a_i^*a_j^*\vec{a}_i\vec{a}_j$. [b] Not refined.

higher than 1 e/Å^3. The slightly oversized thermal parameters relative to those normally observed for Zr–Cl cluster systems are also somewhat elongated along the b direction, the prism axis. This is likely an indication of either an inadequate absorption correction or a low-quality crystal associated with the difficulties in obtaining this compound in crystalline form, as discussed previously.

$Li_6Zr_6Cl_{18}H$. One quadrant of data collected on a Syntex diffractometer at room temperature (Table I) was corrected for absorption using one ψ-scan and averaged for space group $R\bar{3}$ selected on the basis of axial photos and diffraction conditions. The Zr atom was located by analysis of the Patterson map. An electron density map calculated after a brief refinement (ALLS[18]) revealed three new sets of peaks, each with about one-third of the electron density of Zr, and these were assigned as Cl atoms. Refinement of these anisotropically and the variation of a secondary extinction coefficient led to a difference Fourier map in which peaks of about 2 e/Å^3 and in reasonable positions could be assigned to a single set of Li atoms. The residuals reached 2.2% and 2.6%, respectively, after further isotropic refinement of lithium. Refinement of its occupancy to 84 (3)% was accompanied by a decrease in the isotropic thermal parameter from 3.7 (2) to 2.6 (3) Å^2, but the residuals did not change significantly. The validity of this result is doubtful as it would reduce the electron count to an unprecedented level of 12. (See also contrary evidence under Syntheses.) Lithium at full occupancy could also be refined anisotropically but the B_{ii} values were similar (2.5–3.5) and differed by $<2\sigma$. The final difference map was flat to ≤ 0.5 e/Å^{-3}.

Properties. Proton NMR studies were conducted as before.[12] For ^{7}Li studies, about 40 mg of $\geq 95\%$ $Li_6Zr_6Cl_{18}H$ was sealed into a Pyrex tube ca. 0.7 × 1.0 cm. Spectra of the static sample were collected on a Bruker WM-200 spectrometer at 116.6 MHz. Magnetic susceptibilities were measured at 10 kG on a Quantum Design MPMS SQUID magnetometer over the range of 6–300 K.

Results and Discussion

The atom and isotropic-equivalent temperature parameters for $Rb_4Zr_6Cl_{18}C$ and $Li_6Zr_6Cl_{18}H$ are listed in Table II, while important distances and angles are given in Table III. Further data collection and refinement information, anisotropic atom displacement parameters, and structure factor results for both structures are given in the supplementary material.

$Rb_4Zr_6Cl_{18}C$. The phase is clearly isostructural with $K_4Nb_6Cl_{18}$[8] save for the carbon atom. The centered $Zr_6(C)Cl_{12}Cl_6$ clusters form pseudo-close-packed slabs in the (001) plane with the Rb atoms spread along the surface of these layers, as shown in the [100] and [001] projections in Figures 1 and 2, respectively. The lack of superposition of the rubidium atoms in these reflects the β angle of 115°. The clusters possess C_{2h} symmetry and have normal dimensions for a carbon-centered zirconium chloride units.[2] Deviations of individual Zr–Zr distances from their average by 0.007 Å or less are presumably connected with a packing (matrix)

(18) Lapp, R. L.; Jacobson, R. A. USDOE Report IS-4708, 1979.

Table III. Important Distances (Å) and Angles (deg)

$Rb_4Zr_6Cl_{18}C$		$Li_6ZrCl_{18}H$	
	Distances		
Zr1–C (×2)[a]	2.2939 (6)	(Zr–H)	(2.257)
Zr2–C (×4)	2.2831 (4)		
Zr1–Zr2 (×4)	3.2409 (6)	Zr–Zr (×6)	3.1975 (8)
Zr1–Zr2 (×4)	3.2319 (7)	Zr–Zr (×6)	3.1856 (7)
Zr2–Zr2 (×2)	3.2292 (6)		
Zr2–Zr2 (×2)	3.2283 (4)		
$\bar{d}$	3.2338	$\bar{d}$	3.1916
Zr–Cl[i]			
Zr1–Cl3 (×4)	2.551 (1)	Zr–Cl1 (×6)	2.5532 (9)
Zr1–Cl4 (×4)	2.528 (1)	Zr–Cl1 (×6)	2.560 (1)
Zr2–Cl1 (×4)	2.538 (1)	Zr–Cl2 (×6)	2.5671 (9)
Zr2–Cl2 (×4)	2.545 (1)	ZrCl2 (×6)	2.576 (1)
Zr2–Cl3 (×4)	2.545 (1)		
Zr2–Cl4 (×4)	2.521 (1)		
$\bar{d}$	2.538 (1)	$\bar{d}$	2.564
Zr–Cl[a]			
Zr1–Cl5 (×2)	2.564 (2)	Zr–Cl3 (×6)	2.687 (1)
Zr2–Cl6 (×4)	2.606 (1)		
$\bar{d}$	2.592		
Rb–Cl2	3.577 (1)	Li–Cl1	2.669 (9)
Rb–Cl3	3.4987 (9)		2.804 (9)
	3.780 (1)	Li–Cl2	2.605 (9)
Rb–Cl5	3.115 (1)	Li–Cl3	2.430 (9)
Rb–Cl6	3.188 (2)		2.500 (9)
	3.287 (1)		2.563 (9)
	3.186 (2)		
$\bar{d}$	3.376	$\bar{d}$	2.595
	Angles		
Zr2–Cl1–Zr2 (×2)	79.00 (4)	Zr–Zr–Zr	59.80 (1)
Zr2–Cl2–Zr2 (×2)	78.74 (5)		
Zr1–Cl3–Zr2 (×4)	78.99 (4)	Cl1–Zr–Cl1	89.59 (4)
Zr1–Cl2–Zr2 (×4)	79.60 (4)	Cl1–Zr–Cl2	166.76 (3)
av	79.15	Cl1–Zr–Cl2	167.20 (3)
Cl3–Zr1–Cl4 (×2)	169.74 (5)	Cl1–Zr–Cl3	81.60 (3)
Cl1–Zr2–Cl2 (×2)	168.84 (3)	Cl1–Zr–Cl3	82.14 (3)
Cl3–Zr2–Cl4 (×2)	168.82 (4)		
av	169.14	Zr–Cl1–Zr	76.89 (3)
		Zr–Cl2–Zr	77.67 (3)
		Cl1–Li–Cl2	170.4 (4)
		Cl1–Li–Cl3	173.3 (4)
		Cl2–Li–Cl3	81.0 (2)
		Cl2–Li–Cl3	86.9 (3)
		Cl3–Li–Cl3	161.42 (4)
		Cl3–Li–Cl3	104.8 (3)
		Cl3–Li–Cl3	91.81 (3)

[a] Frequency per cluster.

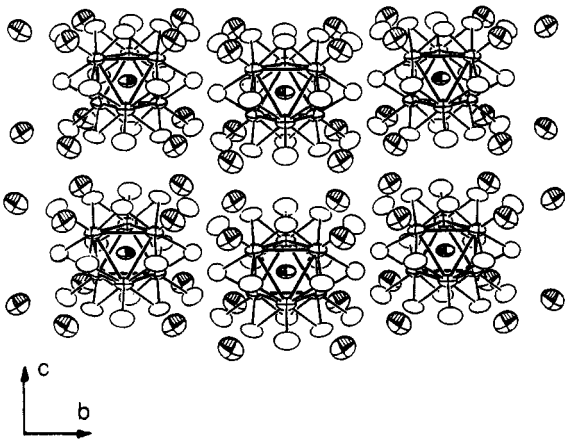

Figure 1. [100] section of the structure of $Rb_4Zr_6Cl_{18}$, showing two cluster layers along $\vec{c}$. The carbon atoms are represented by the small quarter-shaded thermal ellipsoids, while rubidium atoms are the large shaded elements. Zirconium and chlorine atoms are crossed and open (90% probably) ellipsoids, respectively. Carbon lies at the intersection of a 2-fold axis along b and the perpendicular mirror plane (space group $C2/m$).

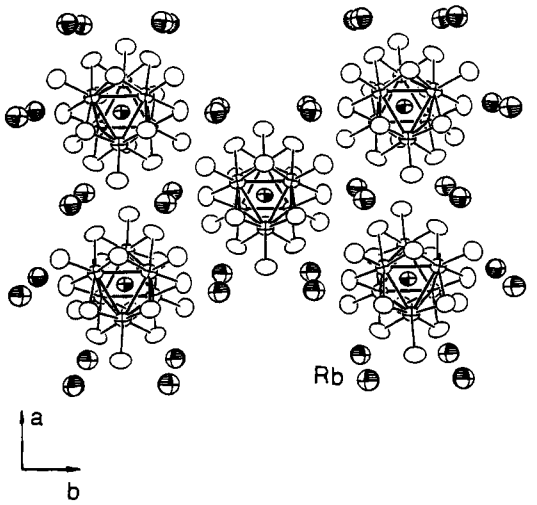

Figure 2. [001] view of one centered cluster layer and the surrounding cations in $Rb_4Zr_6Cl_{18}C$ with the same atom identifications as in Figure 1. The offsets in rubidium and therefore in the layer stacking parallel the β angle, 115°.

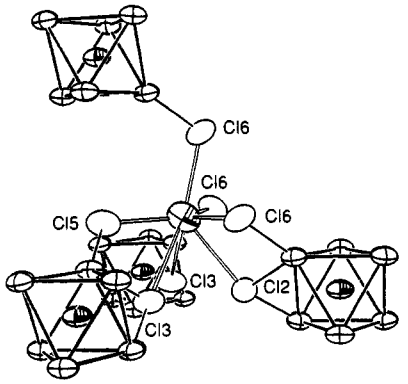

Figure 3. Environment of rubidium in $Rb_4Zr_6Cl_{18}C$, $\vec{c}$ vertical. Note the uneven bonding of the cation to the horizontal cluster layers.

effects rather than electronically driven, since this is a normal 14-electron cluster.

A noteworthy feature is the shortness of the exo Zr–Cl^a bonds in $Rb_4Zr_6Cl_{18}C$, which are the smallest among all $M_xZr_6Cl_{18}Z$ examples, 0.08 Å less than even those in $Rb_5Zr_6Cl_{18}B$,[2] where the packing seems much more favorable. These bonds are more polar than Zr–Cl^i within the cluster and therefore are more directly influenced by cluster connectivity and the number and nature of the neighboring countercations. In this case, the relatively low ratio of cations per $Zr_6Cl_{18}Z$ cluster as well as the relatively low field of Rb^+ both contribute to the shorter Zr–Cl^a distances. For the same reason, the two Zr–Cl^a distances differ from each other by 0.04 Å as their coordination numbers are not equal (Cl5, 1 Zr + 2 Rb; Cl6, 1 Zr + 3 Rb). Phenomena of this character are repeatedly observed throughout zirconium chloride cluster systems, and arguments utilizing simple ionic interactions work particularly well in the 6–18 family where there is no direct interconnection of clusters. The general tendency for the more polar Cl^a–cation contacts to be shorter, and more numerous, than Cl^i–cation values (Table III) is also evident.

The single type of Rb^+ occurs in a general position, and its coordination polyhedron is rather asymmetric as a result of both its nature and the arrangement of clusters and cations required by the stoichiometry. Each Rb^+ is surrounded by four clusters in a pseudotetrahedral fashion (Figure 3). Three clusters from one layer form the base of the tetrahedron, contributing three closer Cl^a (Cl5, Cl6) atoms in a triangular plane about the cation and three more distant Cl^i. A single Cl^a (Cl6) from the adjacent layer caps this fragment at a somewhat greater distance. The Rb–Cl^a distances are at least 0.2 Å shorter than the Rb–Cl^i type. The average distance to the seven nearest chlorine atoms is 3.376 Å, or 3.309 Å if the longest Rb–Cl3 is omitted, in good agreement with the sum of crystal radii, 3.37 Å for CN7 or 3.33 Å for CN6.[19]

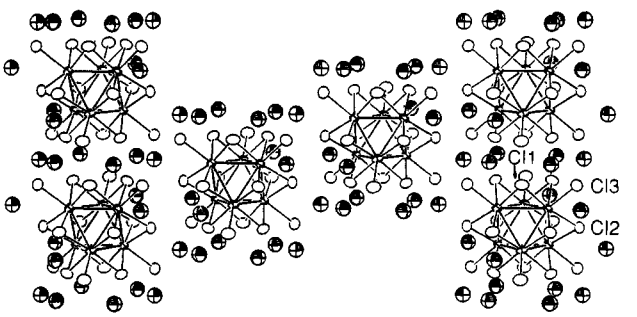

Figure 4. Approximate [110] view of layers of $Zr_6(H)Cl_{12}Cl_6$ clusters (outlined) in rhombohedral $Li_6Zr_6Cl_{18}H$ with the layers of lithium between and within these as shaded (90%) ellipsoids ($\vec{c}$ vertical). Hydrogen occupies the nominal center of each cluster ($\bar{3}$ symmetry).

Although each layer of clusters in the $Rb_4Zr_6Cl_{18}C$ lattice is close packed (Figure 2), the stacking of these layers in a similar manner does not follow. This appears to result from the condition that a three-dimensional, close-packed cluster array would generate only two tetrahedral cation sites per cluster whereas the stoichiometry requires four (Figure 3). In accordance, the cluster layers do not stack in a close-packed way; rather they slide with respect to each other to give a β angle of 115°. This peculiar cluster array not only creates the required number of cation sites but also provides reasonable Rb^+–Cl^a interactions. Another result of this arrangement is that the chlorine atoms do not lie in close-packed arrays either. The chlorine sublattice contains close-packed regions in layers parallel to (001) that are associated with a cluster units, but because of the intrusion of the Rb atoms in the same layers, a longer range close-packed chlorine sublattice does not exist.

The electronic driving force associated with the formation of this somewhat less than ideal structural arrangement of 14-electron clusters is remarkable. Given carbon as the essential interstitial element, the stability of a $Zr_6Cl_{18}C$ cluster, and the presence of excess zirconium, the reaction process still rejects the formation of $Rb_5Zr_6Cl_{18}C$ with a 15-electron cluster in the boride structure in favor of this electronically optimal cluster unit in an unusual, and evidently not completely stable, structure. At least the considerable difficulties in gaining crystalline $Rb_4Zr_6Cl_{18}C$ (see Experimental Section, Syntheses) instead of nearly amorphous, probable disproportionation products is less puzzling in light of the structure. In contrast to $Rb_5Zr_6Cl_{18}B$,[2] where the cations that hold the clusters together occur both within the layers (Rb1) and between them (Rb2, Rb3), $Rb_4Zr_6Cl_{18}C$ has only one type of rubidium and this seems to provide distinctly poorer binding between cluster layers, being bonded to one cluster layer much more strongly via three Rb–Cl^a and three Rb–Cl^i interactions than to the other layer where only one Cl^a atom is a close neighbor (Figure 3). However, from a "destructive" point of view, these structural features may make $Rb_4Zr_6Cl_{18}C$ an interesting pseudolayered candidate for intercalation studies. It has already proven to be a useful reactant in room-temperature solution chemistry that leads to, for example, an $(Et_4N^+)_4Zr_6Cl_{18}C^{4-}\cdot 2CH_3CN$ derivative.[13] Its hydrolytic instability greatly distinguishes it from $K_4Nb_6Cl_{18}$[8] and other alkali-metal analogues.[20]

$Li_6Zr_6Cl_{18}H$. This phase can be described as cubic-close-packed $Zr_6(H)Cl_{18}^{6-}$ clusters of D_{3d} symmetry bound together by lithium cations (Figure 4). This arrangement can be readily derived from the rhombohedral $Zr_6Cl_{12}H$ structure ($Zr_6I_{12}C$-type[10]), in which inner chlorine atoms in adjacent clusters occupy all exo positions (Cl^{a-i}), through the addition of both six Cl^a anions to each cluster to open up these bridges and six lithium cations between the clusters. There are 12 lithium atoms at the ends of (along $\vec{c}$ from) each cluster and 6 closer lithiums about the waist, the latter also

(19) Shannon, R. D. *Acta Crystallogr.* **1976**, *A32*, 751.
(20) Fleming, P. B.; Mueller, L. A.; McCarley, R. E. *Inorg. Chem.* **1967**, *6*, 1.

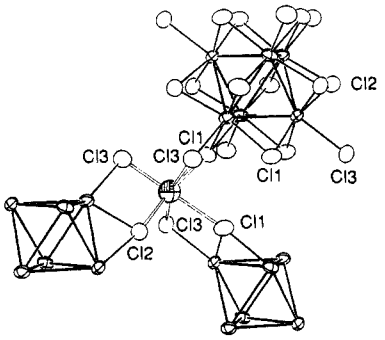

Figure 5. Environment about lithium (shaded) in $Li_6Zr_6Cl_{18}H$. The exo Cl3 is more tightly bound.

being part of those at the ends of adjoining clusters. The arrangement can also be described in terms of cubic-close-packed chlorine layers with intervening mixed layers of zirconium and lithium segregated and ordered in pseudooctahedral holes between them. The metal core of the cluster has dimensions comparable to those in the other structurally characterized, 13-electron, H-centered cluster compound, $K_2ZrCl_6{\cdot}Zr_6Cl_{12}H$.[7] The trigonal compression of the new cluster, with 0.012 Å (11σ) distinguishing the two Zr–Zr distances, is only about one-quarter of that found before, implying that this distortion is a probable result of a matrix, not an electronic, effect. The Zr–Cl^a distance here is almost 0.1 Å longer than in $Rb_4Zr_6Cl_{18}C$ (above) but 0.08 Å shorter than in $K_2ZrCl_6{\cdot}Zr_6Cl_{12}H$. This again reflects the inverse polarizing and bonding effects of the isolated cations on Cl^a: lowest for Rb^+ in the particular $Rb_4Zr_6Cl_{18}C$ arrangement, intermediate for Li^+ here (and Ba^{2+} in $Ba_3Zr_6Cl_{18}Be$[5]), and largest for zirconium(IV) in $ZrCl_6^{2-}$ groups in $K_2ZrCl_6{\cdot}Zr_6Cl_{18}H$, where Cl^a is actually 0.30 Å closer to the isolated zirconium than to a cluster vertex.

Lithium in a general position is surrounded by three cluster units, each contributing one Cl^i and one Cl^a, as shown in Figure 5. The six Li–Cl distances range from 2.430 (9) to 2.804 (9) Å, with an average, 2.595 Å, that is slightly larger than the summation of the crystal radii, 2.57 Å. The coordination polyhedron is highly distorted, implying that the ion plays a lesser role in determining the structure or its stability. The range of Li–Cl distances is also a direct reflection of both the coordination environment and the basicity of each type of chlorine: $Cl3^a$ with 1 Zr + 2 Li neighbors has the shortest, $Cl1^i$ with 2 Zr + 1 Li is intermediate, and $Cl2^i$ with 2 Zr + 2 Li has the longest Li–Cl distance.

Since the dominant interactions between Li^+ and other structure components are polar in nature, the ion also tends to adopt a suitably sized cavity with the fewest cationic second neighbors. The observed site has 3 Zr and 3 Li nearest neighbors (Li–Zr = 3.73–3.99 Å; Li–Li) 3.47–3.84 Å). Two other potential sites with six chlorine neighbors have either 4 Zr and 7 Li (general position, Li–Zr = 3.24–4.38 Å; Li–Li = 3.25–3.98 Å) or 6 Zr and 6 Li neighbors ($\bar{3}$ at 0, 0, $^1/_2$, Li–Zr = 3.65 Å; Li–Li = 3.84 Å). The evident cost of filling the latter two positions and the lack of a good alternative packing must be major factors in prohibiting the formation of compounds like $Li_7Zr_6Cl_{18}H$ with the optimal 14 cluster-based electrons. The unsuccessful substitution of sodium in this structure may be explained by a size factor. Since the lithium occupies six-coordinate positions between the same pair of chlorine layers as do the Zr atoms, and the two have similar radii, replacement of the former with the larger sodium must lead to distortions that destabilize the structure. Besides the cluster electron count, structural limitations such as geometry, packing, and ionic interactions imposed on the solids are important factors that help determine whether a phase is stable or not. It is only when a suitable balance among these factors is achieved that a phase may be obtained from high-temperature solid-state reactions.

The size and some characteristics of the Zr_6H portion of the $Li_6Zr_6Cl_{18}H$ structure are virtually the same as in $K_2ZrCl_6{\cdot}Zr_6Cl_{12}H$ [$=K_2Zr(Zr_6Cl_{18}H)$], the Zr–centroid (H) distance in the new phase, 2.257 Å, being a probably insignificant 0.006 Å

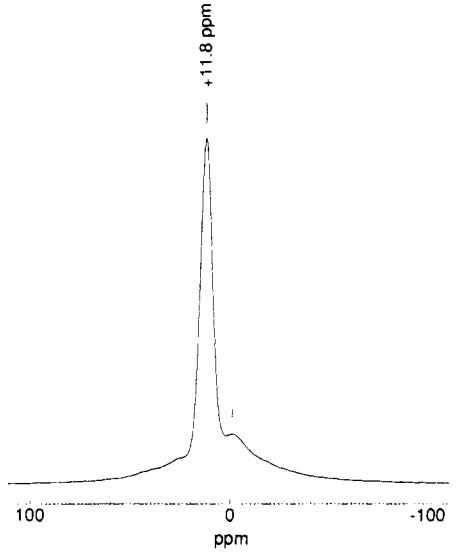

Figure 6. Static ^7Li solid-state NMR spectrum of $Li_6Zr_6Cl_{18}H$ at room temperature relative to LiCl(s).

shorter than in the older. Both are 13-electron cluster examples. The intracluster space is again much too large for tight binding of hydride, which even in tetrahedral coordination has d(Zr–H) in the range of 2.08–2.10 Å.[11]

Other Properties. A high mobility seems reasonable for a hydrogen lying within such an electron-rich zirconium cluster. A ^1H solid-state NMR study of the lithium salt at room temperature and 220 MHz revealed a broad signal at around 400 ppm (with respect to $Fe^{3+}(aq)$), characteristic of a proton in such an environment and comparable to the approximately 500 ppm shift observed for $Zr_6Cl_{12}H$.[12]

Although the single-crystal X-ray analysis of $Li_6Zr_6Cl_{18}H$ succeeded in locating and refining the lithium, confirmation of the results seemed desirable because of its limited scattering of X-rays. Another objective was to accumulate experience in solid-state ^7Li NMR spectroscopy, since no examples of this type could be found in the literature. The room-temperature NMR spectrum of static $Li_6Zr_6Cl_{18}H$ (Figure 6) contains a sharp and narrow peak at +11.8 ppm with respect to LiCl (hwhm = 4.7 ppm). This signal is best described as Lorentzian, in contrast to the broader Gaussian peak (hwhm = 31 ppm) observed for ^7Li ($I = {}^3/_2$) in cubic symmetry in solid LiCl where the nuclei do not experience quadrupole interactions. As the NMR signal from a powder sample should always be symmetrical with respect to the central peak, the small shoulder seen in the spectrum at about 0 ppm (Figure 6) is assigned to LiCl, which could have resulted from incomplete reaction or partial decomposition of the sample while it was being sealed in the container.

The +11.8 ppm shift observed for ^7Li in $Li_6Zr_6Cl_{18}H$ is the largest observed so far in a small group of lithium-containing zirconium chloride cluster phases, viz., −2.2 ppm in $LiZr_6Cl_{14}Mn$[6] and −0.4 ppm in $Li_2Zr_6Cl_{15}Mn$.[4] Although unpredictable contributions could arise from van Vleck (field-induced) paramagnetic effects, the shifts do nicely parallel the expected trend in lithium charge (deshielding) based solely on the relative basicity of its chlorine neighbors. This should increase in the sequence Cl^{i-a}, Cl^i, Cl^{a-a}, Cl^a as these have 2 + 1, 2, 2 more distant, and 1 zirconium neighbors, respectively. The largest downfield shift occurs for $LiZr_6Cl_{14}Mn$ (−2.2 ppm) ($CsZr_6I_{14}C$-type[10] but with the cation in a different site), where lithium occurs in a rather distorted octahedral site with only one Cl^{a-a} neighbor, the remainder being Cl^i atoms. In $Li_2Zr_6Cl_{15}Mn$ (−0.4 ppm), the single type of cation occurs in a site of D_{2h} symmetry with four Cl^i and two Cl^{a-a} (intercluster bridging) neighbors. The ^7Li shift in LiCl with its 6–6 coordination is slightly more positive. Finally, the largest positive shift, 11.8 ppm, occurs in $Li_6Zr_6Cl_{18}H$ where the cation has more polar interactions with three Cl^a and three Cl^i neighbors. Further refinement of this treatment might include

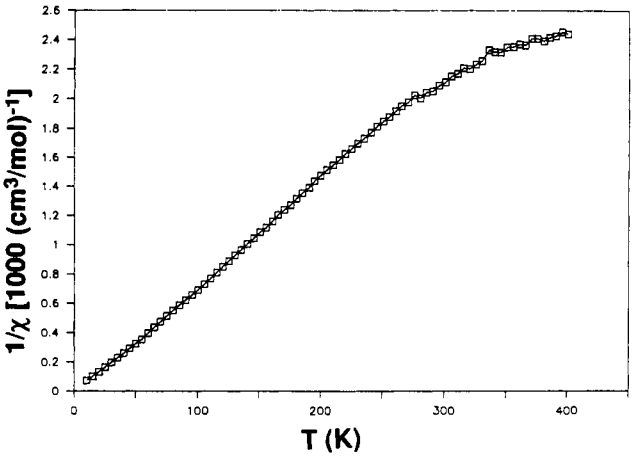

Figure 7. Inverse molar susceptibility of $Li_6Zr_6Cl_{18}H$ as a function of temperature (K) at 10 kG.

the number of and distances to second neighbor zirconium atoms in the clusters.

The lack of detailed features in this spectrum limits further information that can be extracted, namely the asymmetry parameter as well as the quadrupole coupling constant. Spinning of the sample was precluded by the need to work with a sealed glass container. But the simple peak profile observed may be intrinsic for lithium in such a low-symmetry environment.

$Li_6Zr_6Cl_{18}H$ should be paramagnetic because of its 13 cluster electrons, the HOMO being t_{2g}^5,[2] and the compound obeys the Curie–Weiss law between about 60 and 260 K (Figure 7). The slope of this line corresponds to an effective magnetic moment of $\sim$1.12 μB, while similar results for $Li_6Zr_6Cl_{18}D$ (not shown) yield 0.96 μB. These values are smaller than expected for one localized unpaired electron. Although we have not analyzed this quantitatively, the qualitative effects are analogous to those studied for $Zr_6I_{12}Mn$ (t_{2g}^{*1}),[21] the discrepancy probably arising from spin–orbital coupling with the outer zirconium atoms together with delocalization, etc. as reflected in the "orbital reduction factor". The effects should diminish and $\mu\beta$ approach the classical value at higher temperatures, as the data appear to indicate, although measurements above room temperature would be necessary to verify this. Of course, the absolute values of the susceptibilities become very small at higher temperatures and, as shown, less accurately known.

The stabilities and structures of these $A^I_x(Zr_6Cl^i_{12}Z)Cl^a_6$ phases in general are intimately tied to the effective packing of relatively large anions with x smaller cations, the A^I ions in suitably-sized cavities being more strongly bound by Cl^a neighbors. Problems associated with these factors may be responsible for the fact that so few examples of 6–18 cluster phases have been encountered with zirconium. The $M_2M'Zr_6Cl_{18}Z$ family[6,7] clearly involves a better way to do this, larger $M'Cl_6$ units being the formal source of the Cl^a atoms. The marginal stability encountered for $Rb_4Zr_6Cl_{18}C$ with respect to Rb_2ZrCl_6 and an interbridged cluster phase $RbZr_6Cl_{15}C$ (and perhaps other products) is the first example of such an extreme behavior. A low stability is known for the isostructural $A^I_4Nb_6Br_{18}$ phases,[22] but the marginal stability of $(Nb_6Br_{12})Br_n$ clusters in general appears to be the principal reason in these cases. The $[Zr_6(H)Cl_{12}]Cl_{18}^{6-}$ example studied here appears to be stable only with lithium, less reduced $A^i_2ZrCl_6{\cdot}Zr_6Cl_{12}H$ phases being the alternatives. Hydride-centered clusters in phases with other stoichiometries and structures have not appeared by accident, although explorations with this interstitial element have been less intensive. The 13-electron cluster, one electron short of the optimum, is a good example of "something is better than nothing" in the interstitial stabilization found for all zirconium halide clusters.

Acknowledgment. The ^{7}Li NMR data were provided by V. Rutar of the Departmental Instrumentation Services, and those for ^{1}H, by L. Flanagan and B. C. Gerstein. This research was supported by the National Science Foundation, Solid State Chemistry, via Grants DMR-8318616 and -8902954 and was carried out in facilities of the Ames Laboratory, DOE.

Supplementary Material Available: Crystal and refinement details and anisotropic thermal displacement parameters for $Rb_4Zr_6Cl_{18}C$ and $Li_6Zr_6Cl_{18}H$ (2 pages); tables of observed and calculated structure factor results for the same compounds (11 pages). Ordering information is given on any current masthead page.

(21) Hughbanks, T.; Rosenthal, G.; Corbett, J. D. *J. Am. Chem. Soc.* **1988**, *110*, 1511.

(22) Broll, A.; Juza, D.; Schäfer, H. *Z. Anorg. Allg. Chem.* **1971**, *382*, 69.